Efficacy of antibody-based therapies against Middle East respiratory syndrome coronavirus (MERS-CoV) in common marmosets

Neeltje van Doremalen [a,1], Darryl Falzarano [b,1,2], Tianlei Ying [c,1,3], Emmie de Wit [b], Trenton Bushmaker [a], Friederike Feldmann [d], Atsushi Okumura [b,e], Yanping Wang [c], Dana P. Scott [d], Patrick W. Hanley [d], Heinz Feldmann [b], Dimiter S. Dimitrov [c,**], Vincent J. Munster [a,*]

[a] Virus Ecology Unit, Laboratory of Virology, Division of Intramural Research, National Institute of Allergy and Infectious Diseases, National Institutes of Health, Rocky Mountain Laboratories, Hamilton, MT, USA
[b] Disease Modeling and Transmission, Laboratory of Virology, Division of Intramural Research, National Institute of Allergy and Infectious Diseases, National Institutes of Health, Rocky Mountain Laboratories, Hamilton, MT, USA
[c] Protein Interactions Section, Cancer and Inflammation Program, Center for Cancer Research, National Cancer Institute, National Institutes of Health, Frederick, MD, USA
[d] Rocky Mountain Veterinary Branch, Division of Intramural Research, National Institute of Allergy and Infectious Diseases, National Institutes of Health, Rocky Mountain Laboratories, Hamilton, MT, USA
[e] Department of Microbiology, University of Washington, Seattle, WA, USA

ARTICLE INFO

ABSTRACT

Cases of Middle East respiratory syndrome coronavirus (MERS-CoV) continue to be identified and with a lack of effective clinical treatment and no preventative strategies, treatment using convalescent plasma or monoclonal antibodies (mAbs) is a potential quick route to an intervention. Passive immunotherapy via either convalescent plasma or mAbs has proven to be effective for other infectious agents. Following infection with MERS-CoV, common marmosets were treated with high titer hyperimmune plasma or the mAb m336, at 6 and 48 h post inoculation. Both treatments reduced signs of clinical disease, but reduction in viral loads in the respiratory tract were only found in the hyperimmune plasma group. A decrease in gross pathology was found only in the mAb-treated group, but no histological differences were observed between treated and control animals. While both hyperimmune plasma and the m336 treatments reduced the severity of disease in the common marmoset, neither treatment resulted in full protection against disease.

© 2017 Published by Elsevier B.V.

1. Introduction

Middle East respiratory syndrome coronavirus (MERS-CoV) was first detected in 2012 in a resident of Saudi Arabia, and has since resulted in > 1900 cases with a case fatality rate of 36% (WHO, 2015). The severity and the epidemic potential of MERS-CoV highlights the importance of the development of treatment options. As of yet, no specific vaccine or antiviral treatment against MERS-CoV is available. Few studies have been published investigating the effectiveness of existing antiviral treatments, and no treatments have been thoroughly assessed in clinical trials as of yet.

Convalescent plasma has been identified by the World Health Organization (WHO) and the International Severe Acute Respiratory and Emerging Infection Consortium (ISARIC) as a potential treatment against MERS-CoV to reduce clinical consequences of MERS-CoV infection (2013, WHO, 2014) and recently a study protocol was developed to investigate the feasibility of convalescent plasma treatment in MERS patients (Arabi et al., 2015). In vivo, the administration of convalescent sera obtained from dromedary camels resulted in dose-dependent decreased lung viral titers and

disease severity in an adenovirus-hDPP4 mouse model (Zhao et al., 2015).

Several monoclonal antibodies (mAbs) have been developed against MERS-CoV, which show neutralizing capacity *in vitro* (Jiang et al., 2014; Tang et al., 2014; Ying et al., 2014). Efficacy of mAbs has been assessed in several MERS-CoV mouse models generally showing reduction in virus replication (Corti et al., 2015; Li et al., 2015; Pascal et al., 2015; Luke et al., 2016). These studies suggest that mAbs have potential as MERS-CoV treatment.

The mAb m336, identified from a large phage-displayed antibody library panned against recombinant MERS-CoV spike protein receptor binding domain, inhibited 90% MERS-CoV pseudovirus infection at a concentration of 0.039 μg/ml (Ying et al., 2014). m336 was shown to almost completely overlap with the binding site of DPP4 and mimic critical interactions between DPP4 and the MERS-CoV spike protein (Modjarrad et al., 2016). It has therefore been speculated that the potential for viral escape mutants might be limited by the requirement of the spike protein to bind to DPP4 (Ying et al., 2015). Prophylactic treatment with m336 resulted in significantly reduced viral titer in rabbit lung tissue (Houser et al., 2016) and both prophylactic and therapeutic treatment with m336 protected mice against lethality by MERS-CoV infection (Agrawal et al., 2016). Here we assess the effect of treatment with marmoset-derived hyperimmune plasma as well as the human mAb m336 on disease outcome in the recently developed marmoset MERS-CoV infection model, which recapitulates severe respiratory disease (Falzarano et al., 2014).

2. Materials and methods

2.1. Ethics statement

Approval of animal experiments was obtained from the Institutional Animal Care and Use Committee at Rocky Mountain Laboratories. All experiments were performed in an Association for Assessment and Accreditation of Laboratory Animal Care-approved facility by certified staff, following the guidelines and basic principles in the United States Public Health Service Policy on Humane Care and Use of Laboratory Animals, the NIH Guide for the Care and Use of Laboratory Animals and the Animal Welfare Act, United States Department of Agriculture. The Institutional Biosafety Committee (IBC) approved work with infectious MERS-CoV strains under BSL3 conditions. Sample inactivation was performed according to IBC-approved standard operating procedures for removal of specimens from high containment.

2.2. Generation of MERS-CoV hyperimmune sera

Hyperimmune plasma was obtained from a convalescent common marmoset (*Callithrix jacchus*) from a previous experiment (Falzarano et al., 2014) inoculated with 5.2×10^6 TCID$_{50}$ MERS-CoV via the intratracheal, intranasal, ocular and oral route, then inoculated with 5.2×10^6 TCID$_{50}$ MERS-CoV on 20 dpi via the intratracheal route and finally inoculated with 5.2×10^6 TCID$_{50}$ MERS-CoV adjuvated with Titermax Gold (Sigma Aldrich) on 41 dpi via the intramuscular route. The final virus neutralizing (VN) titer was 3840. This method was chosen as sera collected after the initial infection did not contain sufficient neutralizing antibodies (VN titer = 40). As a control, plasma was obtained from an uninfected common marmoset (internal collection), VN titer <20.

2.3. Study design

The common marmoset MERS-CoV infection model was used; MERS-CoV infection results in the development of more severe respiratory disease than observed in the rhesus macaque model (de Wit et al., 2013; Munster et al., 2013; Falzarano et al., 2014). Common marmosets were procured from an USDA-approved source (Worldwide Primates Inc). Animals were monitored for the presence of disease by clinical observation and serology for the presence of disease at Worldwide Primates Inc. Additionally, when animals arrived at Rocky Mountain Laboratories they were placed in quarantine and clinically evaluated by serum chemistry, complete blood counts and thoracic radiography to confirm absence of previous infection.

Three different groups were created; the hyperimmune plasma group (H), the monoclonal antibody group (M), and the control group (C). Three animals were randomly assigned per group and inoculated as described previously (Falzarano et al., 2014). Briefly, inoculation with MERS-CoV strain EMC/2012 was performed intranasally (100 μl per nare), orally (500 μl), intratracheally (500 μl) and ocular (50 μl per eye) with DMEM containing 4×10^6 TCID$_{50}$ MERS-CoV/ml (total dose 5.2×10^6 TCID$_{50}$). The hyperimmune plasma and monoclonal antibody groups, consisting of one female and two male common marmosets each, received 1 ml hyperimmune plasma or m336 diluted in PBS (5 mg/ml) intravenous (I.V.) at 6 hpi, and 1 ml hyperimmune plasma or m336 subcutaneous (S.C.) at 2 dpi (marmosets H1-3, M1-3). Two out of three animals in the control group (all male common marmosets), received 1 ml control plasma I.V. 6 hpi, and 1 ml control plasma S.C. 2 dpi (marmosets C1-2). The third animal received 1 ml of PBS (diluent of the mAb) via the same routes (marmoset C3). The animals were observed twice daily for clinical signs of disease, using a scoring system as described previously (Falzarano et al., 2014). Breathing was scored as normal (<60/minute), increased (60–100/minute), or severely increased (>100/minute). Based on the scoring sheet, euthanasia was indicated at a clinical score of 35 or more. Clinical exams were performed on 0, 2, 5, and 7 dpi on anaesthetized animals using isoflurane and ketamine. X-rays were taken and nasal, oral, fecal, and urogenital swabs were collected in 1 ml DMEM with 50 U/ml penicillin and 50 μg/ml streptomycin. Blood samples were collected on −5, 2, and 7 dpi and examined using the Piccolo Xpress chemistry analyzer (Abaxis). The blood sample collected on 2 dpi was obtained before treatment was administered. Temperature was monitored with IPTT-300 temperature probes (BMDS) that were injected interscapularly prior to the start of the experiment. All animals were euthanized at 7 dpi (Fig. 1A). Terminal blood samples were obtained and samples of the following tissues were collected: conjunctiva, nasal mucosa, tonsil, trachea, four lung lobes, mediastinal lymph node, liver, spleen, kidney, and bladder. Gross pathology (surface area of the lung which was either consolidated and/or hyperemic) per lung lobe was documented as percentage area affected by lesions.

2.4. Radiography

Radiographic images acquired included ventrodorsal, right lateral and left lateral thoracic images. Thoracic radiographs were obtained using a mobile digital radiography unit with a flat panel digital detector (Sound Technologies tru/DR, Sound-Eklin Carlsbad, CA). Each set of radiographs was graded according to a published scoring paradigm (Brining et al., 2010) as follows: 0, normal examination; 1, mild interstitial pulmonary infiltrates; 2, moderate interstitial infiltrates, perhaps with partial cardiac border effacement and small areas of pulmonary consolidation (alveolar patterns and air bronchograms); 3, pulmonary consolidation as the primary lung pathology, seen as a progression from grade 2 lung pathology. Grading per animal was done independently and blinded by two veterinarians.
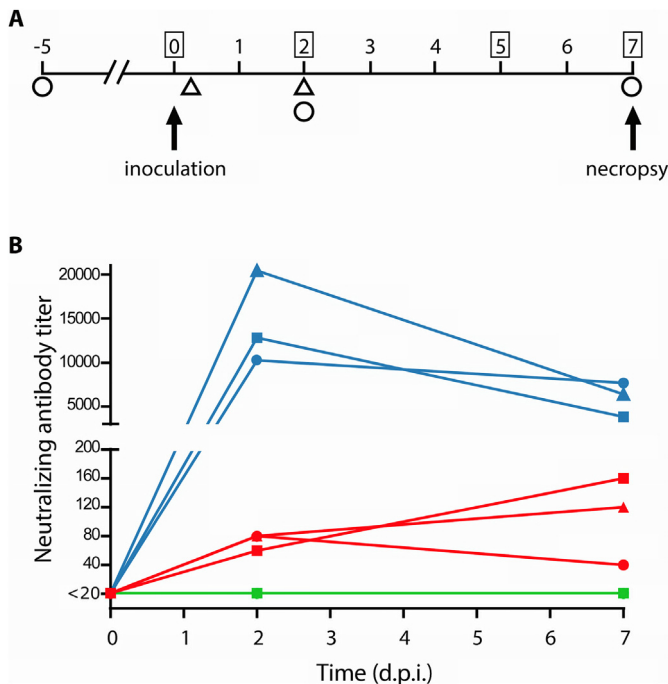
Fig. 1. Experimental schedule and neutralizing antibody titers. (A) The experimental schedule is depicted for all animals per day. □ = Examination; ○ = blood withdrawal; Δ = treatment. (B) Neutralizing antibody titers of marmoset serum samples against MERS-CoV strain HCoV-EMC/2012. Red = Hyperimmune plasma-treated marmosets; Blue = mAb-treated marmosets; Green = control marmosets; ● = 1; ■ = 2; ▲ = 3. (For interpretation of the references to colour in this figure legend, the reader is referred to the web version of this article.)

2.5. Virus and cells

HCoV-EMC/2012 was provided by the Erasmus Medical Center, Rotterdam, The Netherlands. Virus propagation was performed in VeroE6 cells (provided by the Bowen laboratory, Colorado State University) in DMEM supplemented with 2% fetal calf serum, 1 mM L-glutamine, 50 U/ml penicillin and 50 μg/ml streptomycin (2% DMEM). VeroE6 cells were maintained in DMEM supplemented with 10% fetal calf serum, 1 mM L glutamine, 50 U/ml penicillin and 50 μg/ml streptomycin.

2.6. Histopathology and immunohistochemistry

Marmoset tissues were evaluated for pathology and the presence of viral antigen. All tissues were fixed for a minimum of 7 days in 10% neutral-buffered formalin and subsequently embedded in paraffin. Lungs were perfused with 10% formalin and processed for histologic review. The lung is divided into right upper, right lower, left upper, and left lower lobe. Each of these four sections are then sampled at the hilus, at mid-lobe and at the periphery of the lobe for a minimum of 12 sections per animal. This method is used for all non-human primate studies at Rocky Mountain Laboratories. Hereafter, tissue sections were stained with hematoxylin and eosin. For the detection of viral antigen immunohistochemistry was performed using an in-house produced rabbit polyclonal antiserum against HCoV-EMC/2012 (1:1000). Grading was done blinded by a board-certified veterinary pathologist. To obtain morphometrical data of immunohistochemistry staining, stained sections were scanned with an Aperio ScanScope XT (Aperio Technologies, Inc., Vista, CA) and analyzed using the ImageScope Positive Pixel Count algorithm (version 9.1). Between 30 and 105 mm squared were evaluated at 2× magnification. The default parameters of the

Positive Pixel Count (hue of 0.1 and width of 0.5) detected antigen adequately.

2.7. RNA extraction

Tissue for RNA analysis was collected in triplicate. Lung tissue was obtained from the hilar and mid-lobe region of the lung. Samples were analyzed independently in duplicate. Tissues (30 mg) were homogenized in RLT buffer and RNA was extracted using the RNeasy method (Qiagen) according to the manufacturer's instructions. RNA was extracted from swabs using the QiaAmp Viral RNA kit on the QIAxtractor.

2.8. Quantitative PCR

The UpE MERS-CoV detection assay was used for the detection of MERS-CoV viral RNA (Corman et al., 2012). 5 μl RNA was tested with the Rotor-GeneTM probe kit (Qiagen) according to instructions of the manufacturer. Dilutions of MERS-CoV with known titer were run in parallel.

2.9. Determination of limit of detection quantitative PCR

Dilutions of *in vitro* transcribed UpE MERS-CoV RNA were run on the digital droplet PCR (Biorad) in quadruplicate to determine genome copies. Hereafter, dilutions were run on the Rotor-GeneTM in quadruplicate. The last dilution to give a Ct-value in all replicates was defined as the limit of detection (LOD) in genome copies. Finally, the number of genome copies was determined in the MERS-CoV dilutions with known titer, and LOD was calculated in $TCID_{50}$ equivalent.

2.10. Infectious virus titration

Small tissue samples (up to 100 mg) in 1 ml of 2% DMEM were homogenized. Hereafter, MERS-CoV was titrated in quadruplicate in VeroE6 cells; cells were inoculated with ten-fold serial dilutions of tissue homogenate, incubated 1 h at 37 °C, washed twice with PBS, and scored for cytopathic effect 5 days later. $TCID_{50}$ was adjusted for tissue weight and calculated by the method of Spearman-Karber.

2.11. Virus neutralization assay

Two-fold serial dilutions of heat-inactivated (30 min, 56 °C) marmoset sera were prepared in 2% DMEM, after which 100 $TCID_{50}$ of MERS-CoV virus was added. After 1hr incubation at 37 °C, virus was added to VeroE6 cells. At 5 dpi, cytopathic effect was scored. The virus neutralization titer was expressed as the reciprocal value of the highest dilution of the serum, which still inhibited MERS-CoV virus replication.

2.12. Statistical analysis

Student's *t*-test (unpaired, one-tailed) was used to test for significance. P values of <0.05 were considered significant. All values are reported as mean ± SD.

3. Results

3.1. Neutralizing antibody levels in the serum of treated and untreated marmosets

The final VN titer of hyperimmune plasma was 3840, control plasma was <20 and m336 was 491530. Animals were inoculated

with 5.2×10^6 TCID$_{50}$ MERS-CoV strain EMC/2012 and treated IV 6 hpi and SC 48 hpi. These two different administration routes were chosen to achieve high systemic bioavailability; I.V. administration immediately results in high circulating neutralizing antibody titers whereas S.C. administration results in a slower systemic distribution of antibodies, therefore allowing a longer bioavailability (Wohlrab, 2015). Animals treated with hyperimmune plasma reached a neutralizing titer between 40 and 160 at 2 dpi and maintained these levels throughout the experiment. Animals treated with m336 reached neutralizing titers between 10,240 and 20,480 at 2 dpi, which decreased to 3840–7680 at 7 dpi. In contrast, serum obtained from animals treated with control plasma or PBS did not contain detectable levels of neutralizing antibodies at any time point (Fig. 1B).

3.2. The effect of antibody-based treatment on clinical disease upon inoculation of marmosets with MERS-CoV

Upon inoculation with MERS-CoV strain EMC/2012, all animals developed clinical disease. Clinical scores of control group animals were found to be higher than clinical scores of treated animals post inoculation (Fig. 2A). No changes in body temperature were observed. All animals showed loss of appetite and decreased activity, often seen combined with a hunched posture. No changes in respiratory rate were reported for treated animals M1 and M2. Increased respiration rate (>60 breaths/minute) was observed in all other animals, and progressed to labored breathing (>100 breaths/minute) in all three control animals (C1-C3) and one treated animal (H1). This was accompanied by open mouth breathing in all control animals, but not H1.

All radiographs were independently and blindly graded by clinical veterinarians (Brining et al., 2010)) and in all views were normal (score = 0) prior to inoculation on day 0. Within the control group, all three animals were graded at 2 at 5 dpi with severe interstitial infiltrates seen early that progressed to pulmonary consolidation within the caudal and middle lung lobes on 7 dpi (score = 3). Both the hyperimmune plasma treatment and the mAb treatment group on average had lower graded radiographs in comparison to the control group. On 7 dpi, one hyperimmune plasma-treated animal was characterized as having grade 1 (H2, mild interstitial pulmonary infiltrates in the left caudal lung lobes), while the remaining two hyperimmune plasma-treated animals had either moderate (H1, grade 2) or severe (H3, grade 3) radiographic signs. One mAb-treated animal had normal radiographic findings (M2, grade 0) throughout the duration of the study, whereas the other two animals (M1, M3) were scored as presenting with mild radiographic findings (grade 1) (Fig. 2B and C and Fig. S1).

Blood chemistry values were investigated using the Piccolo Xpress chemistry analyzer on −5, 2, and 7 days post inoculation. Overall, no apparent differences in measured clinical chemistries were noted between the control and the treated groups. The values of the investigated parameters (BUN, creatinine, ALT, AST, ALP, GGT, total protein, glucose and calcium) were found to be within the normal ranges for marmosets, and no consistent patterns or trends were noted between groups (Fig. S2).

3.3. Respiratory tract pathology in treated and untreated marmosets

Gross pathology of the lungs was scored by a board-certified veterinary pathologist for each lung lobe, both dorsal and ventral. For the control animals, the median percent lesions was 32.5% (C3), 55% (C1) and 67.5% (C2). No abnormal pathological findings were observed in one of the hyperimmune plasma-treated animals (H2), whereas the median of gross pathology of the lungs in the other

two treated animals was 25% (H1) and 77.5% (H3). Animals treated with m336 showed relatively little gross pathology (median = 0% (M1), 2.5% (M2) and 22.5% (M3)). This difference between control and treated animals was found to be significantly different using an unpaired one-tail Student's t-test (Hyperimmune plasma-treated p = 0.0352; MAb-treated p = 0.0007) (Figs. 2c and 3A). As a measure of pulmonary edema and inflammation, lung to body weight ratios were calculated for each animals. No significant differences were observed between the control and hyperimmune plasma-treated group, however the mAb-treated group had a significantly lower lung to body weight ratio than the control group (p = 0.0039) (Fig. 3B).

No histological differences were observed in the severity or nature of the pneumonia or distribution of viral antigen between the control and treated animals. All marmosets, with the exception of one treated marmoset (H2) which developed no lung pathology, developed multifocal to coalescing, moderate to marked subacute bronchointerstitial pneumonia with type II pneumocyte hyperplasia. The adjacent alveolar interstitium was thickened by congestion, edema and fibrin and moderate numbers of macrophages and neutrophils. Alveolar spaces contained moderate to marked numbers of pulmonary macrophages and neutrophils. Immunohistochemistry demonstrated small numbers of pneumocytes and macrophages positive for viral antigen. These cells were predominantly associated with areas of pneumonia (Fig. 3C). No differences in the amount of viral antigen between groups could be found using morphometrical analysis.

3.4. MERS-CoV replication is reduced in hyperimmune plasma-treated marmosets

On 0, 2, 5, and 7 dpi nasal, oropharyngeal, urogenital and fecal swabs were collected and the presence of viral RNA was examined via Quantitative Reverse Transcription Polymerase Chain Reaction (qRT-PCR). Viral RNA presence was often below detection limit, except for two and one nasal swabs for hyperimmune plasma-treated animals and control animals, respectively, and one oral and fecal swab for one control animal on 7 dpi. In all instances, urogenital swabs were negative (Fig. S3).

Upon necropsy of the animals on 7 dpi, 13 tissue samples were collected and the presence of viral RNA in these tissues was analyzed using qRT-PCR. As observed in previous infection of marmosets (Falzarano et al., 2014), the highest viral loads were found in the lower respiratory tract of the animals (Fig. 4A). Viral loads in lung tissues from hyperimmune plasma-treated compared to control animals were found to be significantly lower using a one-tailed unpaired Student's t-test (average of 4.0×10^4 and 1.2×10^6 TCID$_{50}$ equivalent/gram, respectively, p-value = 0.008). This difference was found to be significant even when negative values from animal H2 were excluded from analysis (average of 5.9×10^4 TCID$_{50}$ equivalent/gram, p-value = 0.0263). However, treatment of marmosets with m336 did not significantly reduce viral load in lung tissue (average of 5.4×10^5 and 1.2×10^6 TCID$_{50}$ equivalent/gram, respectively, p-value = 0.0864) (Fig. 4B).

Viral RNA was found in the nasal turbinates, trachea, conjunctiva, tonsils and mediastinal lymph nodes of some but not all animals with no pattern related to treatment. Viral RNA in the liver, spleen, kidney and bladder was below the limit of detection (Fig. 4C). No infectious virus could be found in any tissue samples.

4. Discussion

Currently no specific antivirals or vaccines are approved for MERS-CoV treatment, and limited information is available on the efficacy of potential treatment options *in vivo*. A potential
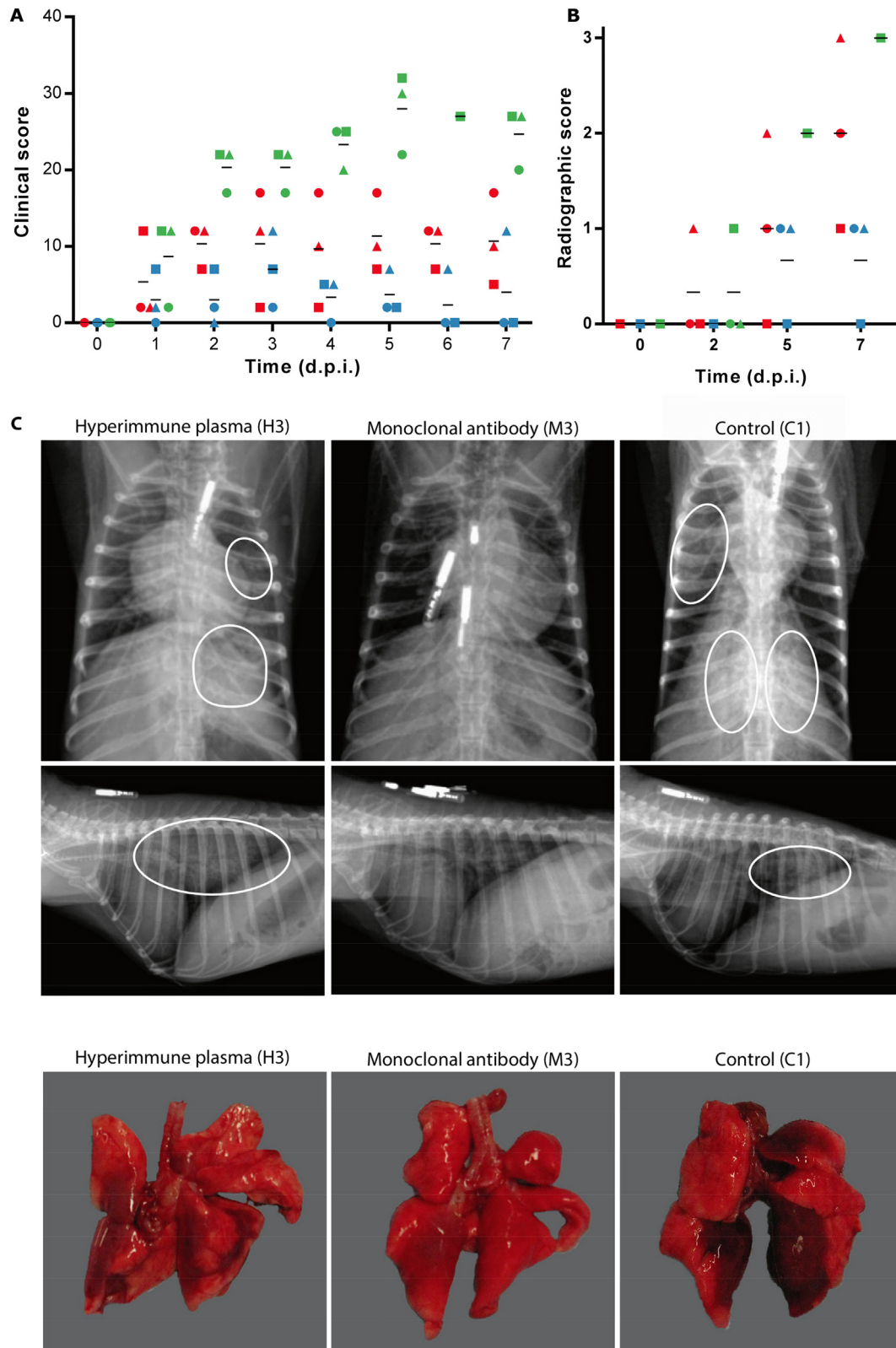
Fig. 2. Disease progression in MERS-CoV infected marmosets. (A) Clinical score of all animals. The animals were observed twice daily for clinical signs of disease and scored using a clinical scoring system prepared for common marmosets (Falzarano et al., 2014). (B) Grading per animal per day was done independently and blinded by two clinical veterinarians. (A/B) Mean values ± SD were calculated. Red = hyperimmune plasma-treated marmosets; Blue = mAb-treated marmosets; Green = control marmosets; ● = 1; ■ = 2; ▲ = 3. (C) Ventral-dorsal and lateral thoracic radiographs as well as gross pathology images of marmosets taken 7 dpi. Shown are animals H3, M1 and C1. (For interpretation of the references to colour in this figure legend, the reader is referred to the web version of this article.)
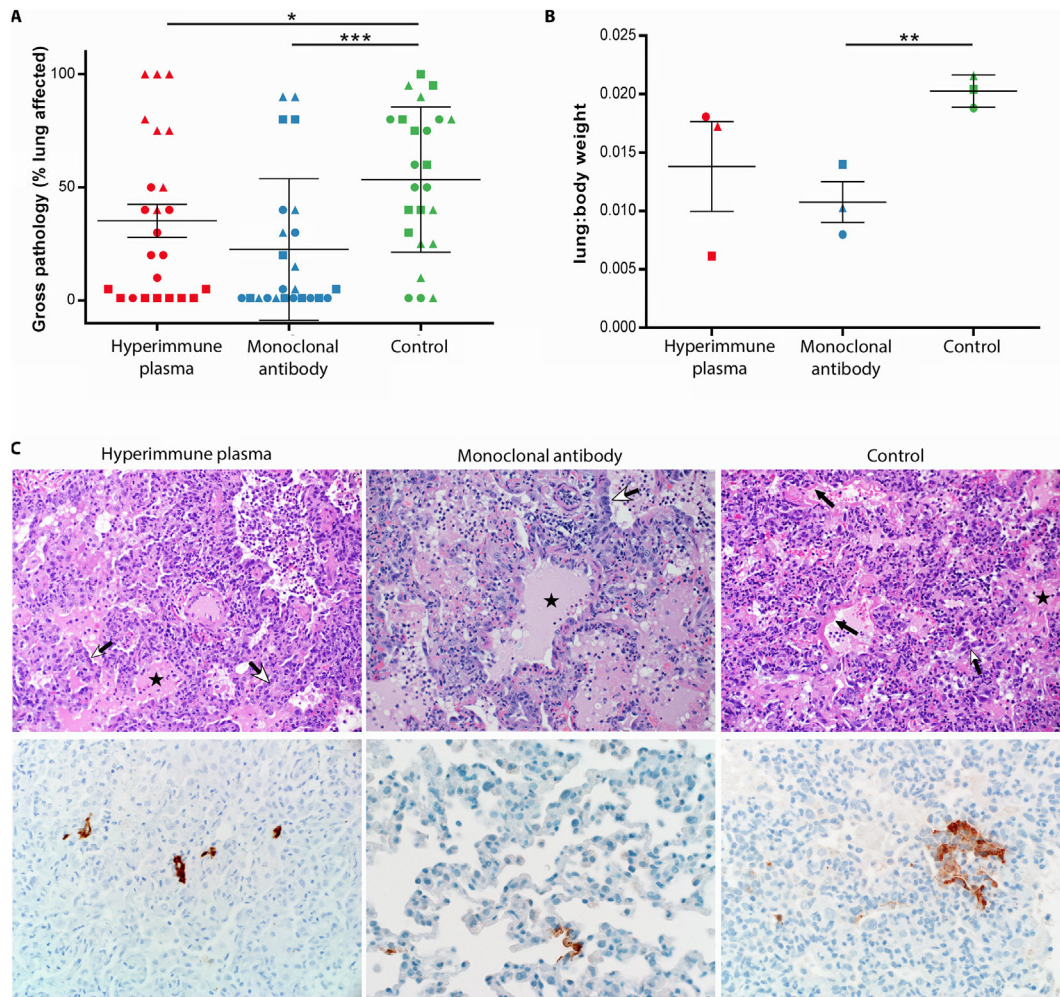
Fig. 3. Pathological changes in the lungs of marmosets. (A) Percentage of area of lung tissue affected by gross lesions was determined on all four lung lobes, both ventral and dorsal sides, resulting in 8 values per animal. Each animal is represented by a different symbol; ● = 1; ■ = 2; ▲ = 3. (B) Lung to body weight ratio was determined as an indicator of lung consolidation. (A/B) Mean values ± SD were calculated. Statistical significance was calculated using a one-tailed unpaired Student's t-test; p-values: *>0.05, ** > 0.01, ***>0.001; Red = hyperimmune plasma-treated marmosets; Blue = mAb-treated marmosets; Green = control marmosets; ● = 1; ■ = 2; ▲ = 3. (C) Lung tissues of hyperimmune plasma-treated animals, mAb-treated animals and control animals were collected on 7 dpi and stained with hematoxylin and eosin (upper panels) or a polyclonal α-MERS-CoV antibody (lower panels). Open arrow = type II pneumocyte hyperplasia; Closed arrow = hyaline membranes; Asterisk = edema, hemorrhage and fibrin. (For interpretation of the references to colour in this figure legend, the reader is referred to the web version of this article.)

treatment for MERS-CoV would be the use of neutralizing antibodies, either via convalescent plasma or monoclonal antibodies. Severity of disease has been associated with a delayed adaptive immune response (Park et al., 2015), and thus antibody-based therapy might be beneficial. Administration of neutralizing antibodies early in disease onset when patients were infected with respiratory pathogens such as SARS-CoV and influenza A virus was reported to be beneficial (Mair-Jenkins et al., 2014). Treatment of SARS-CoV-infected patients with convalescent plasma early in disease progression resulted in a higher likelihood of disease remission and survival (Cheng et al., 2005) and administering convalescent plasma in two SARS-CoV-infected healthcare workers resulted in complete recovery (Yeh et al., 2005). Convalescent plasma treatment of patients with severe A(H1N1)pdm09 influenza virus infection resulted in reduced mortality and respiratory tract viral load (Hung et al., 2011). Meta-analysis of studies on the treatment of Spanish influenza H1N1 1918 with convalescent plasma showed an absolute reduction of 21% in case-fatality rate (Luke et al., 2006).

A recent study suggests that the availability of donors with sufficiently high MERS-CoV antibody titers might be limited; only 12 out of 443 tested sera obtained from patients, healthcare workers and household contacts were positive on ELISA (Arabi et al., 2016). Furthermore, it has been suggested that severity of disease is linked to serological response; in patients who developed severe disease upon infection with MERS-CoV higher neutralizing antibody levels were detected, whereas in patients with mild or subclinical disease lower and potentially short-lived neutralizing antibody levels were detected (Drosten et al., 2014; Park et al., 2015). It has been well-established that severity of disease is linked to the prevalence of comorbidities (Badawi and Ryoo, 2016), the existence of which might contradict the collection of convalescent serum. Thus, the pool of healthy subjects with sufficient neutralizing antibody titer in convalescent plasma might be very limited. Finally, the hyperimmune plasma used in this study had a high neutralizing antibody titer of 3840, whereas at best human convalescent plasma has neutralizing antibody titers of 320—800 (Park et al., 2015; Arabi et al., 2016) (these studies use different methods to measure neutralizing antibodies). It is unclear whether convalescent plasma with lower neutralizing titers would have a similar effect on disease progression, as lower neutralizing antibody titers in the circulation will likely be reached.
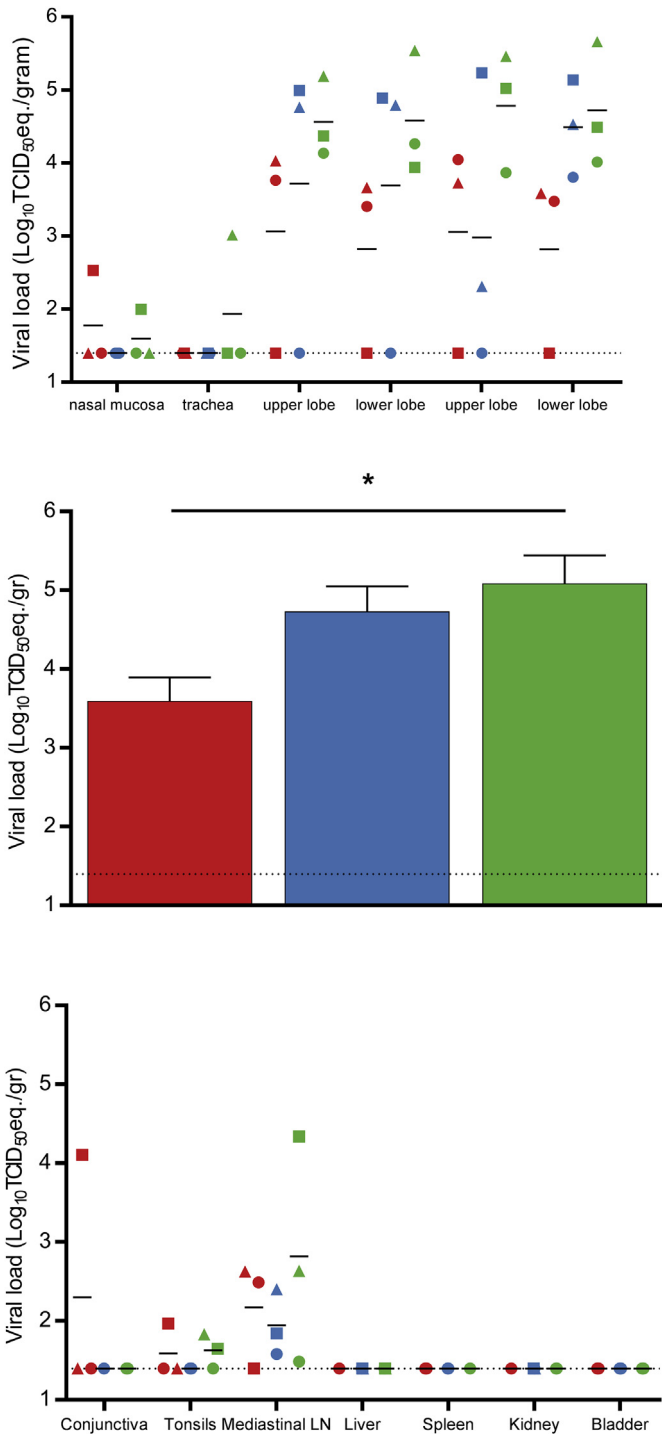
As of yet, very few studies have been done to evaluate the efficacy of convalescent plasma treatment of MERS-CoV. Administration of camel sera to mice sensitized to MERS-CoV infection resulted in a decrease in viral titer in lungs. In addition, when repeating the study with type I interferon receptor-deficient ($IFNAR^{-/-}$) mice, which lose weight upon inoculation with MERS-CoV, a decrease in weight loss as well as less severe histological changes in lung tissue was observed (Zhao et al., 2015). So far, only one documented MERS-CoV case has received convalescent plasma treatment and this patient was still hospitalized on day 77 of illness (Park et al., 2015).

The effect of mAbs against MERS-CoV has been shown both in vitro (Jiang et al., 2014; Tang et al., 2014; Ying et al., 2014) and prophylactic and therapeutic administration of mAbs to MERS-CoV mouse models has been shown to decrease the viral titer and load found in lung tissue (Corti et al., 2015; Li et al., 2015; Pascal et al., 2015; Luke et al., 2016). Prophylactic treatment with m336 via the I.V. or I.N. route resulted in significantly reduced viral titer (40—9000 fold) in rabbit lung tissue. In contrast, administration of m336 1 dpi via the same routes did not reduce viral RNA titers in the lungs of rabbits (Houser et al., 2016). Reduced mortality and morbidity was observed in a MERS-CoV mouse model upon intraperitoneal prophylactic and therapeutic treatment with m336, and therapeutic treatment resulted in a decrease in viral titer as well as viral RNA in lung tissue (Agrawal et al., 2016). It can be argued that neither the rabbit nor the mouse model have a high predictive value for potential MERS therapies in humans. Rabbits remain asymptomatic upon inoculation with MERS-CoV and infection appears to be more prominent in the upper respiratory tract, which suggests that disease progression in rabbits differs considerably from that observed in patients who will require antiviral therapy most (Haagmans et al., 2015). The mouse as a model is valuable as an initial validation method of a therapy, but the predictive value of mouse models for therapeutic applications in humans is relatively limited as opposed to non-human primate models (Seok et al., 2013).

In this study, hyperimmune plasma treatment of marmosets inoculated with MERS-CoV resulted in a small (0.5—1 log) but significant reduction in respiratory tract viral loads, as well as reduced disease severity such as observed with radiographs, compared to marmosets treated with non-convalescent plasma or PBS. However, the observed differences were relatively minimal and no differences in histopathology were observed. In contrast, treatment with m336 in the common marmoset did not result in a significant decrease in respiratory tract viral loads compared to control animals, however a significant reduction in disease severity was observed. This was most pronounced when comparing disease-associated signs. Only one animal treated with m336 showed increased respiratory rates (>60 breaths/minute), and all animals had no evidence of infiltration radiographically, showed decreased levels of gross pathology and the lowest lung to body weight ratio. However, no changes in histology were observed compared to control animals.

qRT-PCR and in situ staining for MERS-CoV were negative in the lungs of one marmoset treated with hyperimmune plasma, although MERS-CoV viral loads and associated pathology were detected in the conjunctiva of this animal. It is possible that in this case, inoculation with MERS-CoV did not result in a successful infection of the respiratory tract. The remaining two marmosets treated with hyperimmune plasma were found to have viral loads of up to 1.1×10^5 TCID$_{50}$ equivalent per gram lung tissue. The marmosets utilized in this study are outbred, and the significance of genetic factors or differences in immunology cannot be excluded. Importantly, when statistical tests were performed excluding the marmoset with no viral load in the respiratory tract, differences in

Fig. 4. MERS-CoV viral loads in tissues of marmosets. (A) Viral load in respiratory tract tissues from marmosets 7 dpi. ● = 1; ■ = 2; ▲ = 3. (B) Mean viral load in lung tissue of marmosets 7 dpi. Mean values ± SD were calculated. Statistical significance was calculated using a one-tailed unpaired Student's t-test; p-values: * > 0.05. (C) Viral load in extra-respiratory tissues from marmosets 7 dpi. Mean values ± SD were calculated. Red = hyperimmune plasma-treated marmosets; Blue = mAb-treated marmosets; Green = control marmosets. Dotted line = Limit of Detection. (For interpretation of the references to colour in this figure legend, the reader is referred to the web version of this article.)

Monoclonal antibodies could provide an alternative; mAb treatment of healthy volunteers inoculated with influenza A virus H3N2 resulted in a reduction in median viral load in nasal swabs and a 35% reduction in median total symptoms (Ramos et al., 2015).

viral load in the lobes of the lower respiratory tract between control and hyperimmune plasma-treated animals were still significant (p = 0.0263).

We show that treatment of MERS-CoV infected animals with hyperimmune plasma or m336 results in lower clinical scores. Treatment with mAbs reduced the occurrence of severe respiratory symptoms further than hyperimmune plasma did, combined with less gross pathology. mAbs might therefore be a better therapy if the goal is to elevate symptoms associated with severe MERS disease. Hyperimmune plasma reduced viral titers, but if a reduction in viral lung load does not result in less severe symptoms, the question is raised of what the importance is of such a change. Regardless, the observed differences are small and most treated animals showed mild-to-moderate respiratory symptoms, suggesting that the effect of both treatments is limited.

Acknowledgments

Appendix A. Supplementary data

Supplementary data related to this article can be found at http://dx.doi.org/10.1016/j.antiviral.2017.03.025.

References

Agrawal, A.S., Ying, T., Tao, X., Garron, T., et al., 2016. Passive Transfer of A Germline-like neutralizing human monoclonal antibody protects transgenic mice against lethal Middle East respiratory syndrome coronavirus infection. Sci. Rep. 6, 31629.

Arabi, Y., Balkhy, H., Hajeer, A.H., Bouchama, A., et al., 2015. Feasibility, safety, clinical, and laboratory effects of convalescent plasma therapy for patients with Middle East respiratory syndrome coronavirus infection: a study protocol. Springerplus 4, 709.

Arabi, Y., Hajeer, A.H., Luke, T.C., Raviprakash, K., et al., 2016. Feasibility of using convalescent plasma immunotherapy for MERS-CoV infection, Saudi Arabia. Emerg. Infect. Dis. 22 (9).

Badawi, A., Ryoo, S.G., 2016. Prevalence of comorbidities in the Middle East respiratory syndrome coronavirus (MERS-CoV): a systematic review and meta-analysis. Int. J. Infect. Dis. 49, 129–133.

Brining, D.L., Mattoon, J.S., Kercher, L., LaCasse, R.A., et al., 2010. Thoracic radiography as a refinement methodology for the study of H1N1 influenza in cynomolgus macaques (Macaca fascicularis). Comp. Med. 60 (5), 389–395.

Cheng, Y., Wong, R., Soo, Y.O., Wong, W.S., et al., 2005. Use of convalescent plasma therapy in SARS patients in Hong Kong. Eur. J. Clin. Microbiol. Infect. Dis. 24 (1), 44–46.

Corman, V.M., Eckerle, I., Bleicker, T., Zaki, A., et al., 2012. Detection of a novel human coronavirus by real-time reverse-transcription polymerase chain reaction. Euro Surveill. 17 (39).

Corti, D., Zhao, J., Pedotti, M., Simonelli, L., et al., 2015. Prophylactic and post-exposure efficacy of a potent human monoclonal antibody against MERS coronavirus. Proc. Natl. Acad. Sci. U. S. A. 112 (33), 10473–10478.

de Wit, E., Rasmussen, A.L., Falzarano, D., Bushmaker, T., et al., 2013. Middle East respiratory syndrome coronavirus (MERS-CoV) causes transient lower respiratory tract infection in rhesus macaques. Proc. Natl. Acad. Sci. U. S. A. 110 (41),

16598–16603.

Drosten, C., Meyer, B., Muller, M.A., Corman, V.M., et al., 2014. Transmission of MERS-coronavirus in household contacts. N. Engl. J. Med. 371 (9), 828–835.

Falzarano, D., de Wit, E., Feldmann, F., Rasmussen, A.L., et al., 2014. Infection with MERS-CoV causes lethal pneumonia in the common marmoset. PLoS Pathog. 10 (8), e1004250.

Haagmans, B.L., van den Brand, J.M., Provacia, L.B., Raj, V.S., et al., 2015. Asymptomatic Middle East respiratory syndrome coronavirus infection in rabbits. J. Virol. 89 (11), 6131–6135.

Houser, K.V., Gretebeck, L., Ying, T., Wang, Y., et al., 2016 May 15. Prophylaxis with a MERS-CoV-specific human monoclonal antibody protects rabbits from MERS-CoV infection. J. Infect. Dis. 213 (10), 1557–1561.

Hung, I.F., To, K.K., Lee, C.K., Lee, K.L., et al., 2011. Convalescent plasma treatment reduced mortality in patients with severe pandemic influenza A (H1N1) 2009 virus infection. Clin. Infect. Dis. 52 (4), 447–456.

Jiang, L., Wang, N., Zuo, T., Shi, X., et al., 2014. Potent neutralization of MERS-CoV by human neutralizing monoclonal antibodies to the viral spike glycoprotein. Sci. Transl. Med. 6 (234), 234–259.

Li, Y., Wan, Y., Liu, P., Zhao, J., et al., 2015. A humanized neutralizing antibody against MERS-CoV targeting the receptor-binding domain of the spike protein. Cell Res.

Luke, T., Wu, H., Zhao, J., Channappanavar, R., et al., 2016. Human polyclonal immunoglobulin G from transchromosomic bovines inhibits MERS-CoV in vivo. Sci. Transl. Med. 8 (326), 326ra321.

Luke, T.C., Kilbane, E.M., Jackson, J.L., Hoffman, S.L., 2006. Meta-analysis: convalescent blood products for Spanish influenza pneumonia: a future H5N1 treatment? Ann. Intern Med. 145 (8), 599–609.

Mair-Jenkins, J., Saavedra-Campos, M., Baillie, J.K., Cleary, P., et al., 2014 Jan 1. The effectiveness of convalescent plasma and hyperimmune immunoglobulin for the treatment of severe acute respiratory infections of viral etiology: a systematic review and exploratory meta-analysis. J. Infect. Dis. 211 (1), 80–90.

Modjarrad, K., Moorthy, V.S., Ben Embarek, P., Van Kerkhove, M., et al., 2016. A roadmap for MERS-CoV research and product development: report from a World Health Organization consultation. Nat. Med. 22 (7), 701–705.

Munster, V.J., de Wit, E., Feldmann, H., 2013. Pneumonia from human coronavirus in a macaque model. N. Engl. J. Med. 368 (16), 1560–1562.

Park, W.B., Perera, R.A., Choe, P.G., Lau, E.H., et al., 2015. Kinetics of serologic responses to MERS coronavirus infection in humans, South Korea. Emerg. Infect. Dis. 21 (12), 2186–2189.

Pascal, K.E., Coleman, C.M., Mujica, A.O., Kamat, V., et al., 2015 Jul 14. Pre- and postexposure efficacy of fully human antibodies against Spike protein in a novel humanized mouse model of MERS-CoV infection. Proc. Natl. Acad. Sci. U. S. A. 112 (28), 8738–8743.

Ramos, E.L., Mitcham, J.L., Koller, T.D., Bonavia, A., et al., 2015. Efficacy and safety of treatment with an anti-m2e monoclonal antibody in experimental human influenza. J. Infect. Dis. 211 (7), 1038–1044.

Seok, J., Warren, H.S., Cuenca, A.G., Mindrinos, M.N., et al., 2013. Genomic responses in mouse models poorly mimic human inflammatory diseases. Proc. Natl. Acad. Sci. U. S. A. 110 (9), 3507–3512.

Tang, X.C., Agnihothram, S.S., Jiao, Y., Stanhope, J., et al., 2014. Identification of human neutralizing antibodies against MERS-CoV and their role in virus adaptive evolution. Proc. Natl. Acad. Sci. U. S. A. 111 (19), E2018–E2026.

WHO, 2014. Position Paper on Collection and Use of Convalescent Plasma or Serum as an Element in Middle East Respiratory Syndrome Coronavirus Response. http://www.who.int/bloodproducts/brn/BRN_PositionPaperConvPlasmaMERSCoV_March2014.pdf.

WHO, 2015. Coronavirus Infections from. http://www.who.int/csr/disease/coronavirus_infections/en/.

WHO and ISARIC, 2013. In: WHO-ISARIC Joint MERS-CoV Outbreak Readiness Workshop: Clinical Management and Potential Use of Convalescent Plasma 10–12 December 2013. http://www.who.int/csr/disease/coronavirus_infections/MERS_outbreak_readiness_workshop.pdf.

Wohlrab, J., 2015. Pharmacokinetic characteristics of therapeutic antibodies. J. Dtsch. Dermatol Ges. 13 (6), 530–534.

Yeh, K.M., Chiueh, T.S., Siu, L.K., Lin, J.C., et al., 2005. Experience of using convalescent plasma for severe acute respiratory syndrome among healthcare workers in a Taiwan hospital. J. Antimicrob. Chemother. 56 (5), 919–922.

Ying, T., Du, L., Ju, T.W., Prabakaran, P., et al., 2014. Exceptionally potent neutralization of Middle East respiratory syndrome coronavirus by human monoclonal antibodies. J. Virol. 88 (14), 7796–7805.

Ying, T., Prabakaran, P., Du, L., Shi, W., et al., 2015. Junctional and allele-specific residues are critical for MERS-CoV neutralization by an exceptionally potent germline-like antibody. Nat. Commun. 6, 8223.

Zhao, J., Perera, R.A., Kayali, G., Meyerholz, D., et al., 2015. Passive immunotherapy with dromedary immune serum in an experimental animal model for middle East respiratory syndrome coronavirus infection. J. Virol. 89 (11), 6117–6120.